R. & M. No. 3775

R. & M. No. 3775

PROCUREMENT EXECUTIVE, MINISTRY OF DEFENCE

AERONAUTICAL RESEARCH COUNCIL

REPORTS AND MEMORANDA

A Time Marching Method for Two- and Three-Dimensional Blade to Blade Flows

By J. D. DENTON

Central Electricity Generating Board

LONDON: HER MAJESTY'S STATIONERY OFFICE

1975

PRICE £2·30 NET

LIST OF CONTENTS

1. Introduction

Time marching methods are in principle the most flexible means of calculating blade-to-blade flows in turbomachinery since the same method can be used for subsonic, transonic and supersonic flows with automatic inclusion of time dependence and shock waves. In practice time marching has not lived up to its promise because large amounts of computer time have been necessary to obtain limited accuracy; times of 5–10 minutes being typical for a 2D problem.

The basic principle of time marching is to start with a guessed flow distribution and integrate the time-dependent equations of motion and energy forward with time until a steady-state solution is obtained. The current 'state of the art' has been reviewed by Gopalakrishnan[1] who concentrates on solving the equations in differential form. An alternative method, described by McDonald,[2] applies the equations for conservation of mass, momentum and energy to elemental control volumes. This integral method is claimed to be more stable than the differential methods since all fluxes are conserved once the steady state is reached. However, as used by McDonald the method requires a complex grid and computer times of the order of 5 minutes.

Stability has always been a problem with time marching, limiting the size of time step which can be taken and hence the number of steps required to obtain a steady state solution. Many means of ensuring stability have been devised for the differential form of the equations. Some of these have been compared by Emery,[3] all achieve stability only at the expense of extra computation. The only method published which does not rely on some form of artificial viscosity or smoothing is that of Marsh & Merryweather.[4] Their method, however, required a very large number of time steps and so, although simple, it was still expensive.

The extension from two to three dimensions is relatively simple in time marching requiring only the solution of an additional momentum equation. However, Gopalakrishnan[1] recently estimated that a 20 hour computer run would be needed to obtain a 3D solution of comparable accuracy to the 2D solutions. Despite this discouragement, time matching seemed to offer the only possibility for solving for transonic flow through highly flared blade rows where the currently available 2D methods are thought to be inadequate. Hence an attempt was made to develop a much faster form of the method.

2. Two-Dimensional Method

The approach chosen was to use McDonald's elemental control volume concept but with a simpler grid. The grid is shown in Fig. 1. It is formed by a series of quasi-streamlines which are evenly spaced in the y direction and by pitchwise lines which need not be evenly spaced in the x direction. The control volumes overlap in the pitchwise direction and calculating points are located at the centre of each element. The quasi-streamlines upstream and downstream of the cascade are chosen to be roughly in line with the flow inlet and outlet directions but these lines do not control the flow direction. Cusps are placed at the leading and trailing edges of the blade to prevent discontinuities in the grid. Periodicity is applied over the bounding quasi-streamlines including cusps and so neither the cusps nor the boundaries exert any force on the flow and do not control its direction. The outlet flow direction is obtained as part of the calculation being determined by the periodicity condition behind the trailing edge.

Throughout the calculation boundary elements are treated exactly as if they were whole elements with half their area beyond the boundary, the fluxes over the face beyond the boundary are found by extrapolation from the boundary and interior points. This is numerically exactly the same as applying the conservation equations to the half element at the wall and then extrapolating from the centre of that element to the boundary. Periodic boundaries are treated in the same way as solid boundaries but after each time step the properties at corresponding points are averaged. Also after each time step the velocities on solid boundaries are resolved parallel and perpendicular to the boundary and the perpendicular component is discarded.

The conservation equations applied to a control volume ΔV for a time step Δt are

$$\text{Mass } \Delta t \,.\, \sum (\rho V_x \,.\, dS_x + \rho V_y \,.\, dS_y) = \Delta V \,.\, \Delta \rho, \tag{1}$$

$$\text{Energy } \Delta t \,.\, \sum (h_0 \rho V_x \,.\, dS_x + h_0 \rho V_y \,.\, dS_y) = \Delta V \,.\, \Delta E, \tag{2}$$

$$x \text{ momentum } \Delta t \,.\, \sum ((P + \rho V_x^2)\, dS_x + \rho V_x V_y \,.\, dS_y) = \Delta V \,.\, \Delta(\rho V_x) \tag{3}$$

and

$$y \text{ momentum } \Delta t \,.\, \sum (\rho V_x V_y \,.\, dS_x + (P + \rho V_y^2)\, dS_y) = \Delta V \,.\, \Delta(\rho V_y). \tag{4}$$

The summations are made over the 4 faces of an element and dS_x, dS_y are the projections of the face in the x and y directions. Also needed is the equation of state

$$P = \rho \,.\, R \,.\, T = \rho \,.\, R(E - \tfrac{1}{2}V^2)/C_v. \tag{5}$$

It is common practice to omit equation (2) and obtain the pressure from the density by assuming isentropic flow. This assumption is not necessarily correct in supersonic flow and will give incorrect predictions for shock waves. A much better means of reducing the number of equations is to assume that the flow takes place with constant stagnation enthalpy. Equations (2) and (5) can then be replaced by

$$P = \rho \,.\, R \,.\, T = \rho \,.\, R(h_0 - \tfrac{1}{2}V^2)/C_p. \tag{6}$$

This assumption becomes exact when the flow becomes steady, even in the presence of shock waves. The unsteady flow is, in effect, being assumed to take place with heat transfer to keep h_0 constant. There is an added advantage in that the speed of a pressure wave at constant h_0 is less than that at constant entropy and so larger time steps can be taken than with the isentropic assumption.

Initially central difference schemes were tried but it was found that a large amount of smoothing was necessary to obtain stability. Study of the mode of instability showed that it was due to combinations of high velocity and low pressure occurring at the centre of an element in conjunction with high pressures and low velocities at the centres of the upstream and downstream elements. This observation suggested a scheme whereby the pressure at the centre of an element acts on its upstream face whilst the velocity at the centre controls the fluxes through the downstream face. When a high x component of velocity arises in an element the mass flux out of the element is increased. This reduces the density and hence the pressure in the element. The reduced pressure acting on the upstream face corrects the initial error in V_x. The fluxes through the quasi-streamlines are small compared to those through the pitchwise lines and are obtained directly from the fluid properties at the calculating points on the streamwise faces of the elements. For the scheme to be effective the equations must be solved in the order: mass–pressure–momentum. The order in which the momentum equations are solved is not important. The procedure adopted is to update the density at all grid points then use the new density in conjunction with the old velocities to obtain the pressure at each grid point (equation (6)). Finally, the new pressures together with the old densities and velocities are used to update the x momentum and y momentum. The method is therefore explicit, in the sense that the new variables are not used in the time step in which they are calculated, with the exception that the new pressure is used immediately it is available.

A simple stability analysis has been developed for the scheme, this is reproduced in the Appendix and predicts that the maximum permissible time step is

$$\Delta t_{\max} = \Delta x_{\min} \,.\, (\sqrt{M^2 + 16} - M)/4c. \tag{7}$$

In practice the maximum stable time step is close to that predicted by equation (7) when $M = 1$ but the increase at low Mach numbers and decrease at high Mach numbers is less than predicted. The pitchwise spacing of the elements has no effect on the stability.

The scheme described above for maintaining stability is equivalent to using upwind differences for mass and momentum fluxes and downwind differences for pressure. A similar scheme was used in differential form by Marsh & Merryweather[4] but appears to have been much less stable than when used with the integral form of the equations. Smoothing is not necessary to stability and in fact reduces the permissible time step. However, the solutions obtained sometimes show a slight 'waviness' with alternate quasi-streamlines having high and low values of the flow properties. This arises because each quasi-streamline is only affected by the difference between properties on its adjacent streamlines and not by the difference between these streamlines and itself. The effect is usually so small as to be scarcely noticeable but if necessary it may be removed by applying a slight smoothing in the pitchwise direction after each time step. Comparisons show that smoothing, several times greater than that needed to remove the waviness, has no significant effect on the surface velocities.

Although simple and highly stable the basic scheme is of limited accuracy. It was therefore modified so that the short term stability is unchanged whilst the steady state solution is determined by more accurate differencing. This was achieved by adding correction factors to the fluxes and pressures at the pitchwise faces of the elements. The correction factors are obtained by curve fits along the quasi-streamlines and changes in them are damped. For example the value of V_x entering element J through its upstream face is taken as

$$V_x \text{ (entering } J) = V_{x,J-1} + CFVX,$$

where after each time step

$$CFVX \text{ (new)} = (1 - RF) \,.\, CFVX \text{ (old)} + RF \,.\, \sum_n a_n \,.\, V_{x,J-n}. \tag{8}$$

The coefficients a_n are determined by the type of curve fit chosen and any curve fit can be used if the value of RF is made low enough (~ 1 per cent). However, it is found that if the correction factors for mass and momentum flux are obtained from an upwind biased curve fit and that for pressure from a downwind biased one, high values of RF can be used. In practice parabolas through J, $J-1$, $J-2$ are used to obtain the fluxes entering element J and a parabola through $J-1$, J, $J+1$ for the pressure on the upwind face of element J. Relaxation factors up to 0·5 can be used without any loss of stability and so the correction factors only lag a few time steps behind the main calculation. In the steady state the gradients at a point are effectively found from a curve fit through 4 points and so, provided the properties vary continuously, the accuracy is equivalent to that of a streamline curvature calculation with the same grid spacing.

The boundary conditions applied at the downstream boundary are a specified uniform static pressure on the last pitchwise line and a condition of zero velocity gradient along the quasi-streamlines. At the upstream boundary the stagnation pressure and temperature and flow direction are specified and there is assumed to be no pressure gradient along the quasi-streamlines. The static pressure on the first pitchwise line is taken to be the same as that calculated on the same quasi-streamline at the second pitchwise line. This static pressure is used in conjunction with an assumption of isentropic flow from the stagnation conditions to calculate the density and velocity. The inlet flow is, therefore, not necessarily uniform.

The method described is very easy to program in 2 dimensions. The complete program requires only about 300 cards and since virtually all operations are arithmetic the computer calculations are very fast. Time requirements are about $1{\cdot}1 \times 10^{-4}$ seconds per point per time step on an IBM 370-165, This compares with a time of $1{\cdot}7 \times 10^{-3}$ seconds on a CDC 3600 quoted by Emery[3] for the fastest of the methods he reviewed. For shock free flow a 30×8 grid is usually adequate, convergence to the steady state is obtained in 300–800 time steps and run times are of the order 10–30 seconds, depending on the number of grid points used. The speed of the method is due to a combination of factors. Firstly, its simplicity makes the computing time per point per time step very low. Secondly, the high stability means that comparatively few time steps are needed to reach a steady state. Finally, the use of a curve fit to obtain the fluxes in the steady state enables comparable accuracy to be obtained with fewer grid points than other methods.

3. Results from the Two-Dimensional Program

The program was developed using the VKI gas turbine blade[5] as a test case since detailed experimental measurements and several other theoretical predictions are available for it. Fig. 3 shows the comparison with experiment at outlet Mach numbers of 0·81 and 1·31. Apart from a failure to predict the sudden decrease in Mach number over the rear of the suction surface at the higher outlet Mach number the agreement is good. None of the other methods used on this blade was able to adequately predict this decrease in velocity which is probably due to a shock meeting the surface. The shock could possibly have been predicted by the present method if more grid points had been used.

The VKI steam turbine blade[5] presents a very severe test of any finite difference scheme since extremely steep gradients of the flow properties occur in both pitchwise and streamwise directions. Using a 10×50 grid gave only fair agreement with experiment but a 20×50 grid gave much better agreement as shown in Fig. 4. The suction peak near the leading edge is predicted more accurately than by any of the other methods whilst only characteristics methods gave significantly better predictions of the shock on the suction surface at the lower Mach number. Again, the shock would have been sharper if more grid points had been used.

Figs. 5 and 6 show comparison with Hobson's[6] two impulse cascades for which accurate analytical solutions are available. These blades are shock free and so it is not surprising that the agreement is good. Fig. 7 shows results for the NASA nozzle blade[8] which is often used as a test case, Gostelow[9] shows comparisons of other methods with this blade. The agreement of the present method with experiment is excellent on the suction surface but there is some discrepancy on the pressure surface near to the blunt leading edge. This error is due to the very rapid changes in flow properties which occur around the leading edge and a finer grid would be needed to give improved accuracy in this region.

To study the behaviour of the calculation in shocked flows it was applied to a convergent–divergent nozzle for which a combined streamline curvature–characteristics solution was available. Fig. 8 shows the result when the nozzle was underexpanded so that an oblique shock is reflected between the walls. The agreement with the characteristics solution is fairly good. Fig. 9 shows the same nozzle with the back pressure raised so that a

strong normal shock forms in it. The curve-fitting scheme cannot follow the rapid changes across the shock so that the discontinuity is smeared over about 4 grid points, irrespective of the grid spacing. The sharp peak in the Mach number distribution before the shock can be prevented by altering the curve-fitting scheme to give upwind mass and momentum fluxes and centred pressures, but the smearing of the shock is slightly worse (Fig. 9). Use of pure upwind differences only enhanced the peak. Although predictions within the shock region are not accurate overall, changes across the shock are correct since mass flow, momentum and energy are conserved across it.

The rate of convergence to the steady state is illustrated for some of the above cases in Fig. 10. It is clear that the flow becomes effectively steady some time before the convergence criterion ($(\Delta V_x/V_x)_{\max} < 0{\cdot}0001$) is reached and that for engineering purposes half the number of time steps would often suffice.

4. Three-Dimensional Method

Extension of the method to three dimensions is straightforward in a Cartesian co-ordinate system requiring only the solving of an additional momentum equation in the third dimension. For turbomachinery problems a 3D calculation is more useful if performed in a cylindrical co-ordinate system so that it can be applied directly to annular blade rows as well as to cascades. This involves some extra geometrical complexity but no extension to the principles of the method.

The mesh used in 3D is formed between planes perpendicular to the axis, meridional quasi stream surfaces equally spaced between the hub and tip and surfaces evenly spaced between the blade suction and pressure surfaces. The intersection of this mesh with a quasi stream surface forms a grid exactly the same as that used in 2D (Fig. 1) and its intersection with a plane containing the axis is shown in Fig. 2.

When applying the conservation equations to an elemented control volume in 3D the continuity, axial momentum and angular momentum equations are solved in a conventional (r, θ, x) cylindrical co-ordinate system. The equations are,

$$\text{Mass } \Delta t \,.\, \sum (\rho V_x \,.\, dS_x + \rho V_\theta \,.\, dS_\theta + \rho V_r \,.\, dS_r) = \Delta V \,.\, \Delta \rho, \tag{9}$$

$$\text{Axial Momentum } \Delta t \,.\, \sum ((P + \rho V_x^2)\, dS_x + \rho V_x V_\theta \,.\, dS_\theta + \rho V_x V_r \,.\, dS_r)) = \Delta V \,.\, \Delta(\rho V_x) \tag{10}$$

and

$$\text{Angular Momentum } \Delta t \,.\, \sum (\rho V_x \,.\, rV_\theta \,.\, dS_x + (P \,.\, r + \rho V_\theta \,.\, rV_\theta)\, dS_\theta + \rho V_r \,.\, rV_\theta \,.\, dS_r) = \Delta V \,.\, \Delta(\rho r V_\theta). \tag{11}$$

When applying the above equations it must be remembered that r and θ are the local radial and tangential directions which vary around the faces of an element and from element to element.

For the radial momentum, however, it is more convenient to use a Cartesian co-ordinate system $(rc, \theta c, x)$ with the radial and tangential directions defined at the centre of each element and remaining unchanged over the whole of that element. This prevents difficulties arising from the V_θ^2/r and $V_r \,.\, V_\theta$ terms which occur when the radial momentum equation is written in cylindrical co-ordinates. The equation becomes

$$\text{Radial Momentum } \Delta t \,.\, \sum (\rho V_x \,.\, V_{rc} \,.\, dS_x + \rho V_{\theta c} \,.\, V_{rc} \,.\, dS_{\theta c} + (P + \rho V_{rc}^2)\, dS_{rc}) = \Delta V \,.\, \Delta(\rho V_{rc}). \tag{12}$$

The pressure is obtained from equation (6) exactly as in two dimensions.

The boundary conditions applied to the 3D problem are also the same as in 2D except that the radial variation of static pressure at the downstream boundary is obtained from radial equilibrium and a condition of zero gradient of radial velocity in the stream-wise direction is applied at the upstream boundary. In all applications to date the upstream total pressure has been taken as uniform but there is no assumption of irrotational flow and non-uniform total pressures can very easily be included. Vorticity shed from the trailing edge of a blade appears as a discontinuity in spanwise velocity at the trailing edge. Since the suction and pressure surfaces effectively feed into the same element downstream of the trailing edge this discontinuity is immediately spread over 3 grid points and at greater distances behind the trailing edge it is further smeared by the coarseness of the grid. This smearing of the discontinuity is an approximation which becomes more exact as the grid spacing is reduced but with the relatively coarse grids which have to be used for 3D flow the smearing influences a considerable proportion of the flow. However, comparison of solutions with different numbers of grid points indicate that the smearing has little effect on the blade-surface pressure distribution. As a future development it may be possible to regard the stagnation streamlines as solid boundaries and to move them as the calculation

proceeds in such a manner as to equalise the pressures at adjacent points. Such a procedure would preserve the discontinuity.

5. Results from the Three-Dimensional Program

The 3D program was found to be no less stable than the 2D version but requires about 3 times as much computer time per point per time step. Computer storage limits the number of calculating points, at present up to 2000 points can be used and this requires 230 k bytes of storage. However, comparison of solutions with differing numbers of grid points has shown that for shock-free problems adequate accuracy can be obtained with about 1000 points. Computer times of 2 to 3 minutes are required with this number of points. It is also interesting that the program can be run with a very coarse grid in the spanwise and pitchwise directions (e.g. 4 points) and this enables qualitative studies of 3D effects to be made reasonably cheaply.

The 3D program can be run as a 2D calculation by making the hub: tip radius ratio very close to unity and in this form it gives results almost identical to the 2D program. There is, however, very little experimental or theoretical data available for comparison with 3D calculations. To obtain some data a 3D duct, representing a turbine nozzle with height variation, was designed and tested. This duct had 60 degrees turning coupled with 50 per cent reduction in height. The pressure distribution along each of its 4 corners was measured at low Mach number and the comparison with the calculated pressure distribution is shown in Fig. 11. The agreement is good over the upstream part of the duct but deteriorates slightly towards the exit. Some of the discrepancy is due to the pressures being measured in the corners of the duct where they are slightly higher than in the free stream.

A further comparison was possible using NGTE data[7] for a cascade of nozzle blades with meridional profiling, the height of the cascade being suddenly reduced by about 15 per cent midway along the blade passage. Fig. 12 shows the calculated and experimental pressure coefficients. Agreement is again fairly good, the very rapid fall in pressure on the suction surface along the curved end-wall is correctly predicted but the heights of the suction peaks are slightly over estimated.

As an example of the application of the method to a transonic annular cascade Fig. 13 shows predictions for the same blade as Fig. 12 but placed in an annular cascade with a flared casing, similar to the one shown in Fig. 2. The hub:tip-radius ratio is 0·75 at outlet and the blade aspect ratio is 2·0 at outlet and 1·50 at inlet. For comparison Fig. 13 also shows a 2D solution at the hub pitch:chord ratio and pressure ratio. It is apparent that 3D effects are small at the hub, being almost entirely due to the increase in stream surface-thickness. Near the casing, however, the pressure distribution is greatly affected by the curvature of the stream surfaces, the load being increased near the leading edge and reduced near the trailing edge.

6. Conclusions

The method developed has proved a rapid and accurate means of calculating blade-to-blade flows. For shock-free flow the two-dimensional method is comparable in speed and accuracy with existing streamline curvature and relaxation methods and in the author's experience it is easier to program and less temperamental than either. For shocked flows time marching provides the only known means of solving simultaneously for mixed subsonic and supersonic flows. All methods smear shock waves over several grid points and so a very fine grid is needed to give accurate results. The speed of the present method means that much more detail can be obtained for the same computing cost.

In three dimensions the method provides a comparatively simple and economical means of obtaining solutions for subsonic flow and is the only known means of solving for transonic flow. Three-dimensional shocked flows can be handled by the present program but will require about 10 minutes of computer time and so have not yet been attempted.

Further developments, which require no extension to the basic principles of the method, include application to three-dimensional rotating-blade rows and to mixed-flow geometries. Ultimately is should be possible to obtain a three-dimensional solution for a complete stage.

REFERENCES

No.	*Author(s)*	*Title, etc.*
1	S. Gopalakrishnan	Fundamentals of time marching—and Application of the time dependent technique of turbomachinery cascades. VKI Lecture Series 59. Transonic Flows in Turbomachinery. May 1973.
2	P. W. McDonald	The computation of transonic flow through two-dimensional gas turbine cascades. A.S.M.E. Paper 71-GT-89.
3	A. F. Emery	An evaluation of several differencing methods for inviscid fluid flow problems. *J. Comp. Phys.* 2, p. 306–331. 1968.
4	H. Marsh and H. Merryweather ..	The calculation of subsonic and supersonic flows in nozzles. Paper 22. Symposium on Internal Flows. University of Salford. April 1971.
5	—	VKI Lecture Series 59. Transonic Flows in Turbomachinery. May 1973.
6	D. Hobson	Shock free transonic flow in turbomachinery cascades. Ph.D. Thesis Cambridge University. Submitted September 1974.
7	R. G. Hoare	Private Communication. NGTE 1974.
8	W. T. Whitney *et al*	Cold air investigation of a turbine for high temperature engine application—Turbine design and overall stator performance. N.A.S.A. TN D-3751. 1967.
9	J. P. Gostelow	Review of compressible flow theories for airfoil cascades. *A.S.M.E. J. Eng. Power.* October 1973.

LIST OF SYMBOLS

$\left.\begin{matrix} x \\ y \end{matrix}\right\}$	Cartesian co-ordinates in 2 dimensions
$\left.\begin{matrix} x \\ r \\ \theta \end{matrix}\right\}$	Cylindrical co-ordinates
$\left.\begin{matrix} x \\ rc \\ \theta c \end{matrix}\right\}$	Cartesian co-ordinates in 3 dimensions with origin at centre of element
C	Blade chord
c	Speed of a pressure wave
C_p	Specific heat at constant pressure
C_v	Specific heat at constant volume
E	Internal energy per unit mass $= C_v T + \frac{1}{2}V^2$
h_0	Stagnation enthalpy $= C_p T + \frac{1}{2}V^2$
M	Local Mach number
M^*	Mach number based on conditions at $M = 1$
P	Pressure
R	Gas constant
S	Projected area of face of element in direction of suffix
T	Temperature
t	Time
Δt	Time step
V	Velocity
ΔV	Volume of element
ρ	Fluid density

APPENDIX

Stability Analysis

Consider flow in a one-dimensional duct divided into elemental control volumes of length Δx and cross-sectional area A. Since the flow across the quasi streamlines is small in comparison with the flow along them such a one-dimensional model should give a good estimate of the stability of a 2D or 3D flow. The flow is assumed to be initially steady but at the start of a time step the velocity at the centre of element J is increased by ΔV_0. The analysis follows the development of this initial perturbation through the time step using the basic scheme whereby the pressure at the centre of an element acts on its upstream face and the velocity at the centre controls the flow through the downstream face.

When solving the continuity equation in the first part of the time step there will be a nett outflow from element J and an equal inflow to element $J + 1$.

$$\Delta m_J = -\Delta m_{J+1} = -\rho \,.\, A \,.\, \Delta V_0 \,.\, \Delta t. \tag{A-1}$$

The resulting changes of density are

$$\Delta \rho_J = -\Delta \rho_{J+1} = -\rho \,.\, \Delta V_0 \,.\, \frac{\Delta t}{\Delta x}. \tag{A-2}$$

The changes in density are immediately used to calculate the change in pressure

$$\Delta P_J = -\Delta P_{J+1} = \left(\frac{\partial P}{\partial \rho}\right) \,.\, \Delta \rho_J = c^2 \left(-\rho \,.\, \Delta V_0 \,.\, \frac{\Delta t}{\Delta x}\right). \tag{A-3}$$

When the momentum equation is now applied to element J there is a nett pressure force $= 2 \,.\, \Delta P_J \,.\, A$ in the x direction and a nett outflow of momentum $= 2\rho \,.\, V \,.\, \Delta V_0 \,.\, A \,.\, \Delta t$. The change of momentum within element J during the next part of time step is

$$\Delta(\rho \,.\, V \,.\, A \,.\, \Delta x) = \left(-2\rho \,.\, c^2 \,.\, \Delta V_0 \,.\, A \,.\, \frac{\Delta t}{\Delta x} - 2\rho \,.\, V \,.\, \Delta V_0 \,.\, A\right) \Delta t, \tag{A-4}$$

i.e.

$$\rho \,.\, \Delta V + V \,.\, \Delta \rho = -2\rho \,.\, c^2 \,.\, \Delta V_0 \,.\, \left(\frac{\Delta t}{\Delta x}\right)^2 - 2\rho \,.\, V \,.\, \Delta V_0 \,.\, \frac{\Delta t}{\Delta x}.$$

Substituting from equation (A-2) for $\Delta \rho$ gives

$$\Delta V = -2c^2 \,.\, \Delta V_0 \,.\, \left(\frac{\Delta t}{\Delta x}\right)^2 - V \,.\, \Delta V_0 \,.\, \frac{\Delta t}{\Delta x}. \tag{A-5}$$

After the time step, the new velocity at the centre of element J is

$$V' = V + \Delta V_0 + \Delta V. \tag{A-6}$$

For stability we must have $|V' - V| < |\Delta V_0|$, i.e.

$$\left|\left(1 - 2c^2 \,.\, \left(\frac{\Delta t}{\Delta x}\right)^2 - V \,.\, \frac{\Delta t}{\Delta x}\right)\right| < 1. \tag{A-7}$$

As Δt is increased instability will start when

$$1 - 2c^2 \,.\, \left(\frac{\Delta t}{\Delta x}\right)^2 - V \,.\, \left(\frac{\Delta t}{\Delta x}\right) = -1,$$

i.e. when

$$2c^2 \cdot \left(\frac{\Delta t}{\Delta x}\right)^2 + \frac{V}{c} \cdot c\frac{\Delta t}{\Delta x} - 2 = 0,$$

i.e.

$$c \cdot \frac{\Delta t}{\Delta x} = -\frac{V}{4c} + \sqrt{\frac{V^2}{16c^2} + 1}$$

or, since $V/c = M$, the local Mach number

$$\Delta t_{\max} = \frac{\Delta x}{4c}\left(\sqrt{M^2 + 16} - M\right), \tag{A-8}$$

Note that $(c \cdot \Delta t)/\Delta x$ is the fraction of a grid space that a pressure wave will travel in one time step.

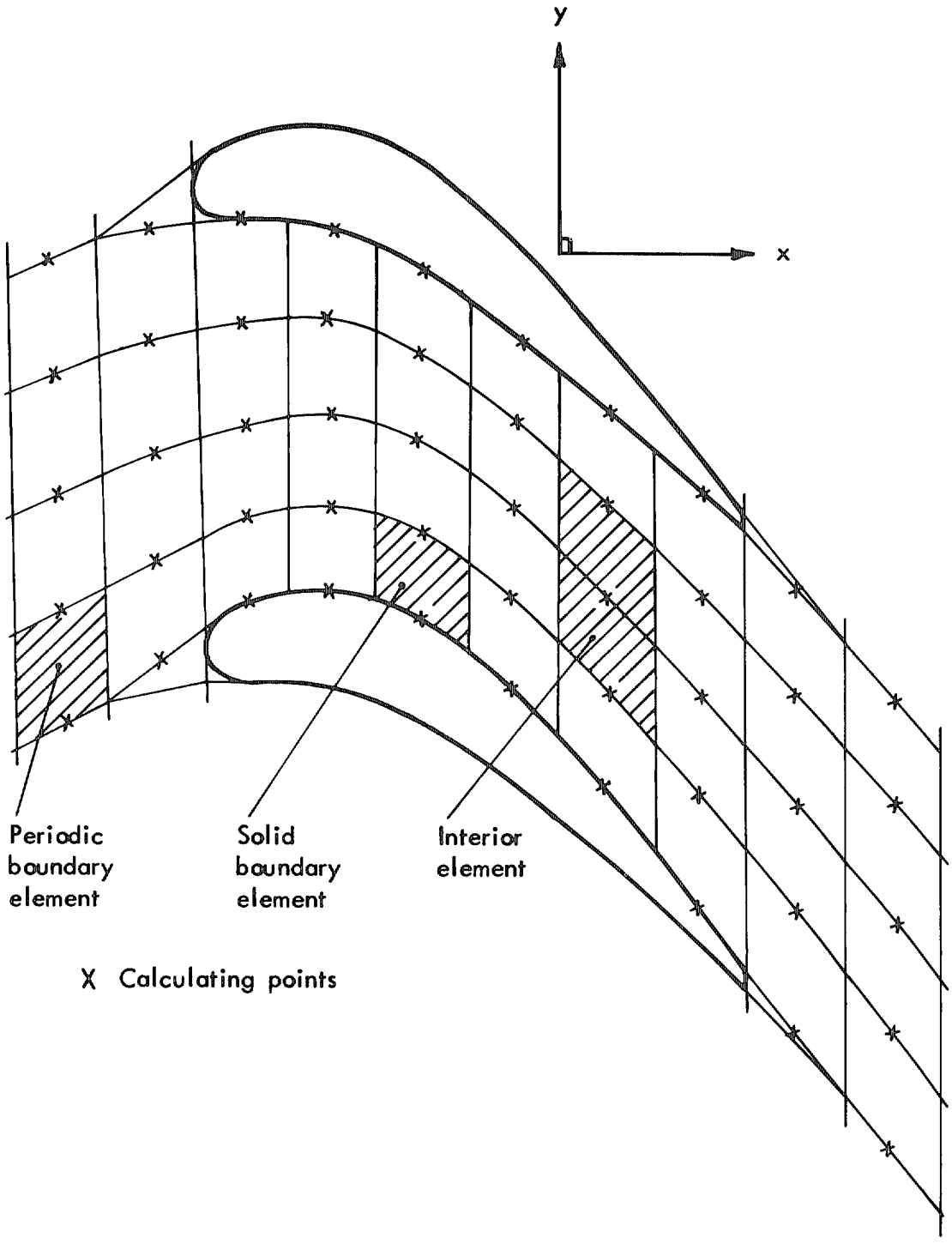

FIG. 1. Grid system in two dimensions. (Grid used is much finer than one shown)

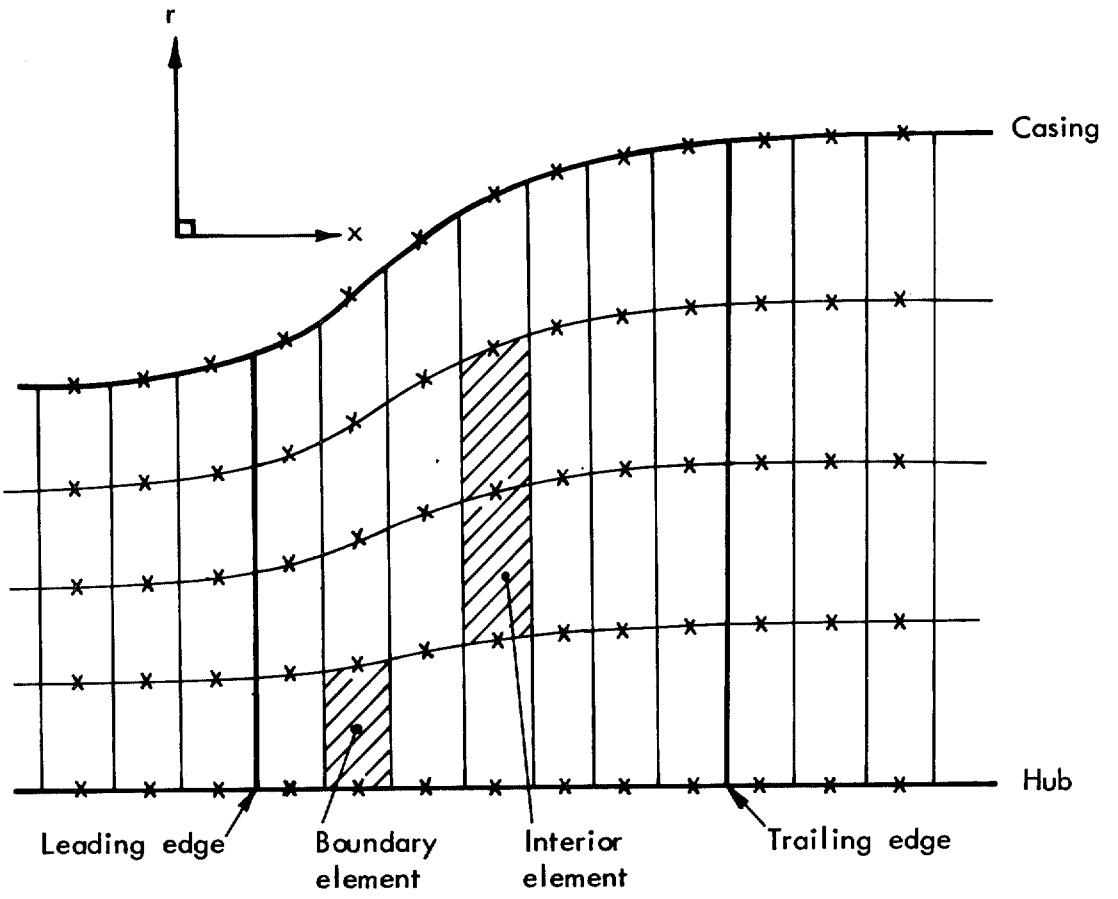

FIG. 2. Intersection of three dimensional grid with meridional plane.

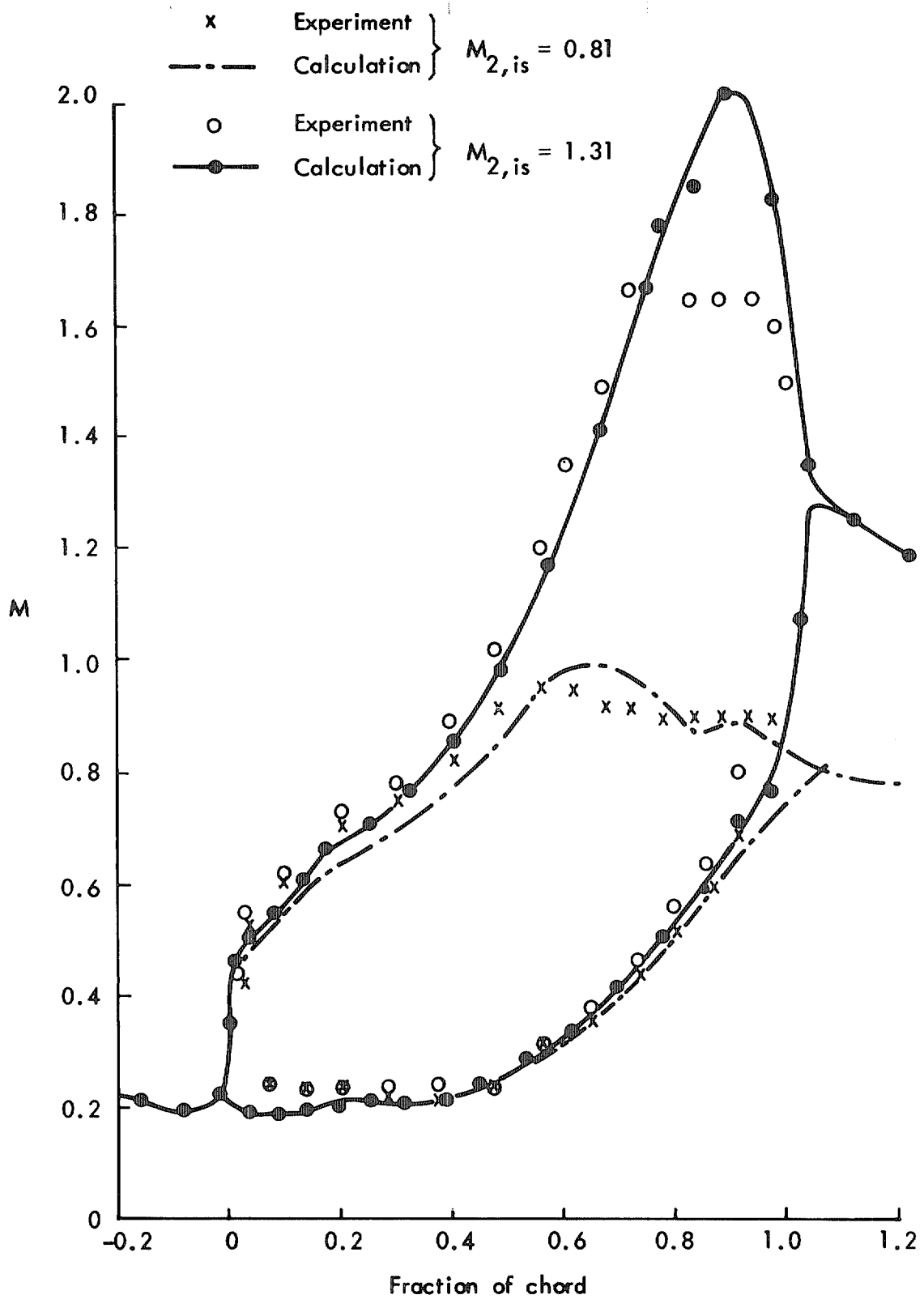

FIG. 3. VKI gas turbine blade.

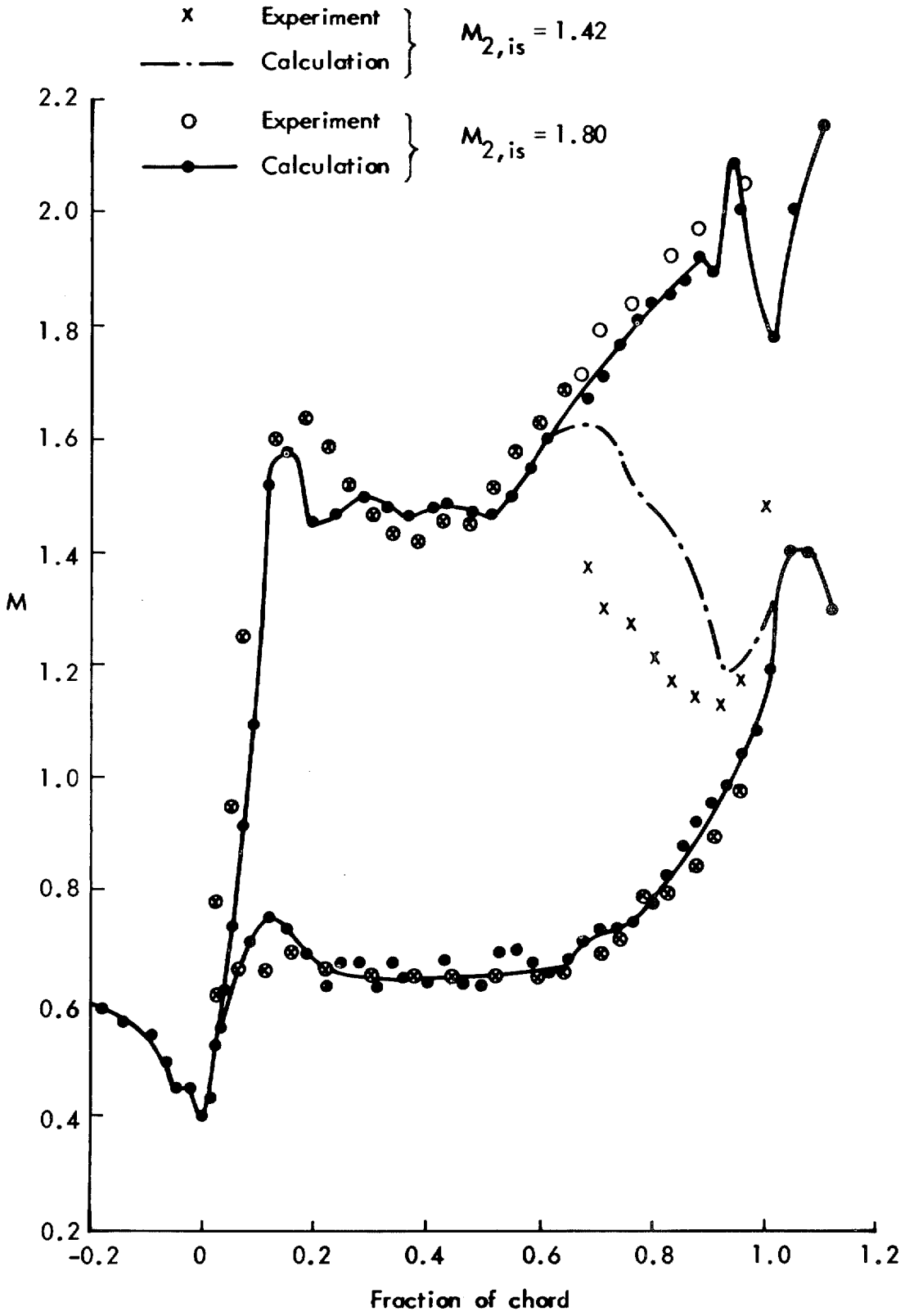

FIG. 4. VKI steam turbine blade.

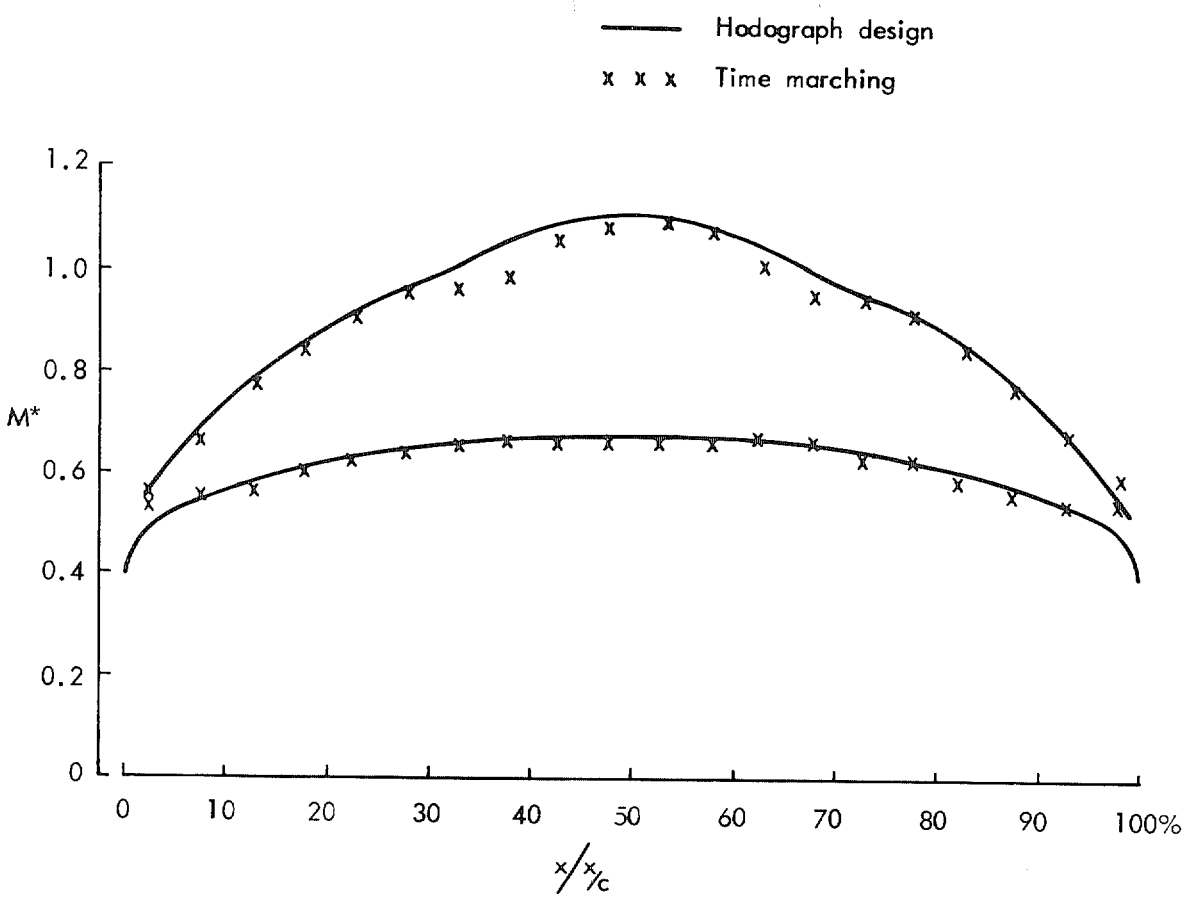

FIG. 5. Hobson's second impulse cascade.

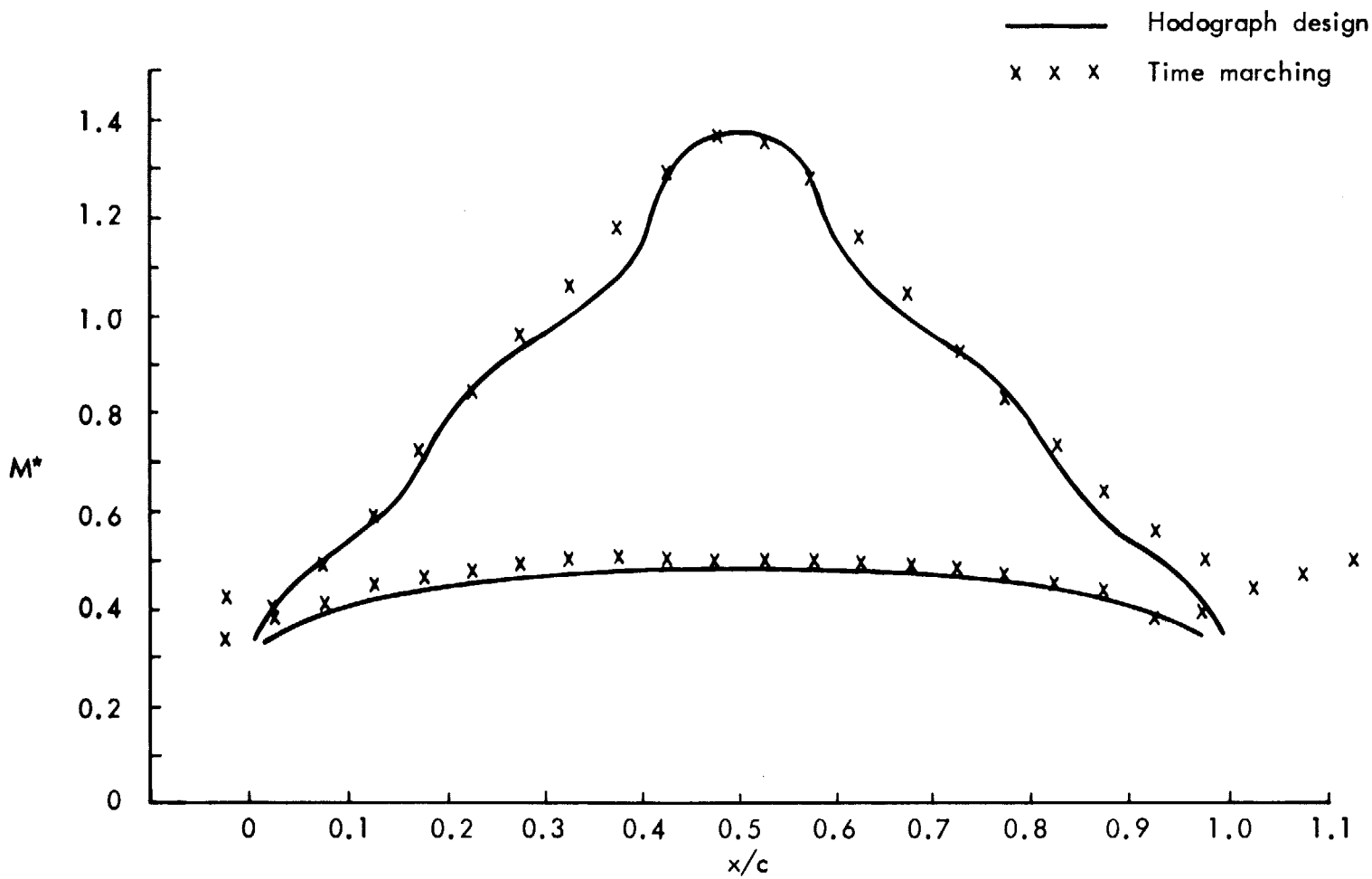

FIG. 6. Hobson's first impulse cascade.

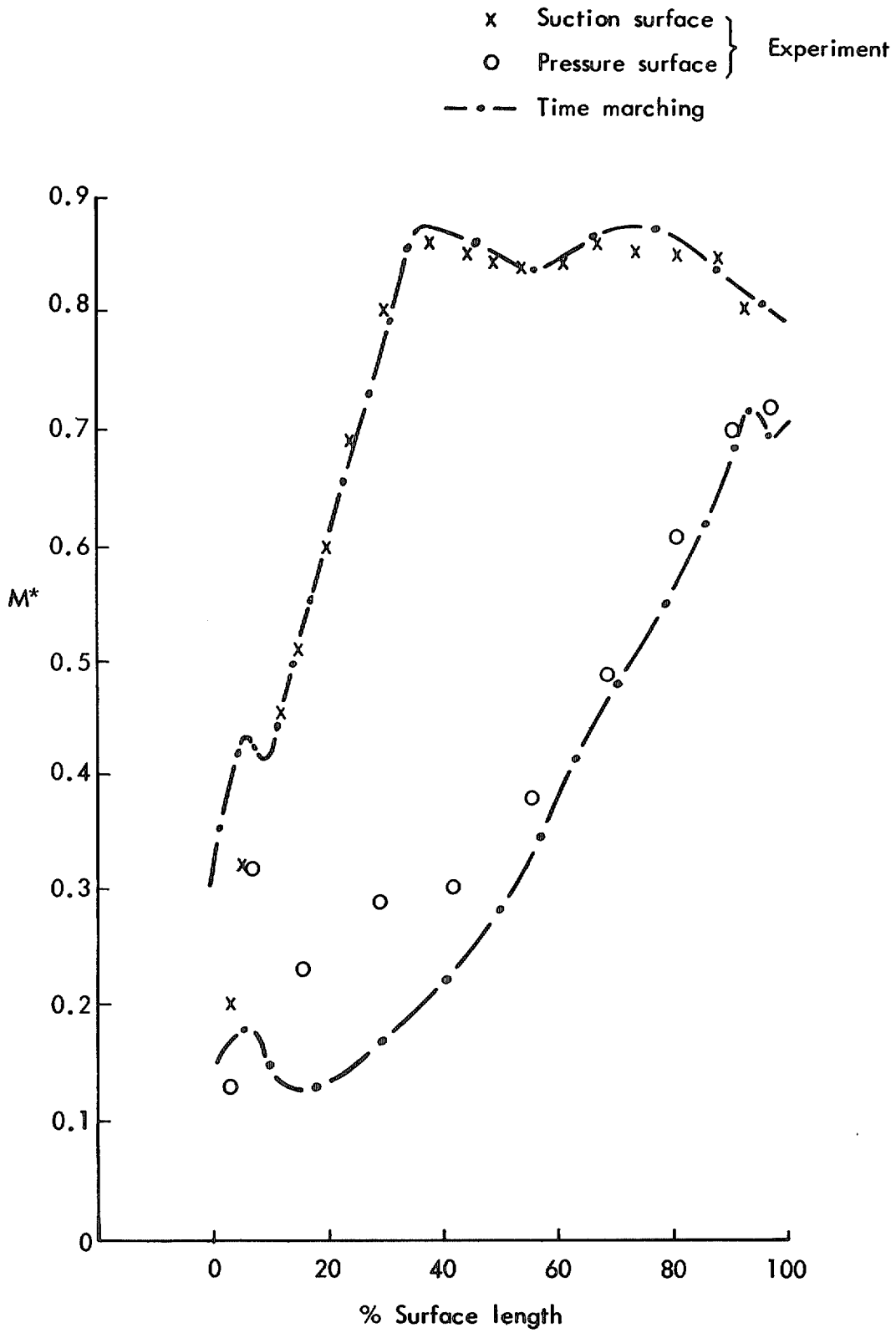

FIG. 7. Nasa Nozzle blade—mean section

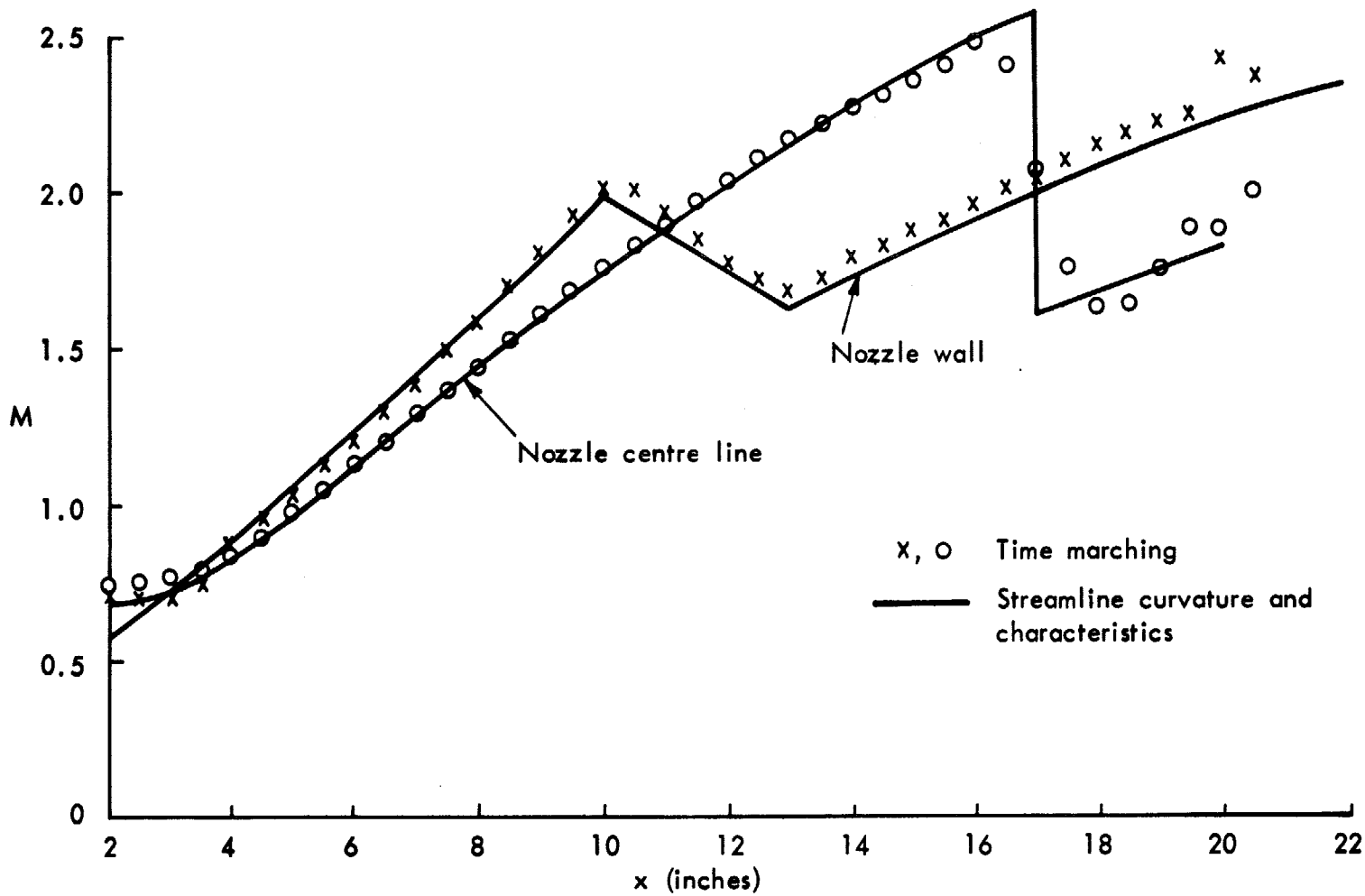

FIG. 8. Convergent—divergent nozzle—underexpanded.

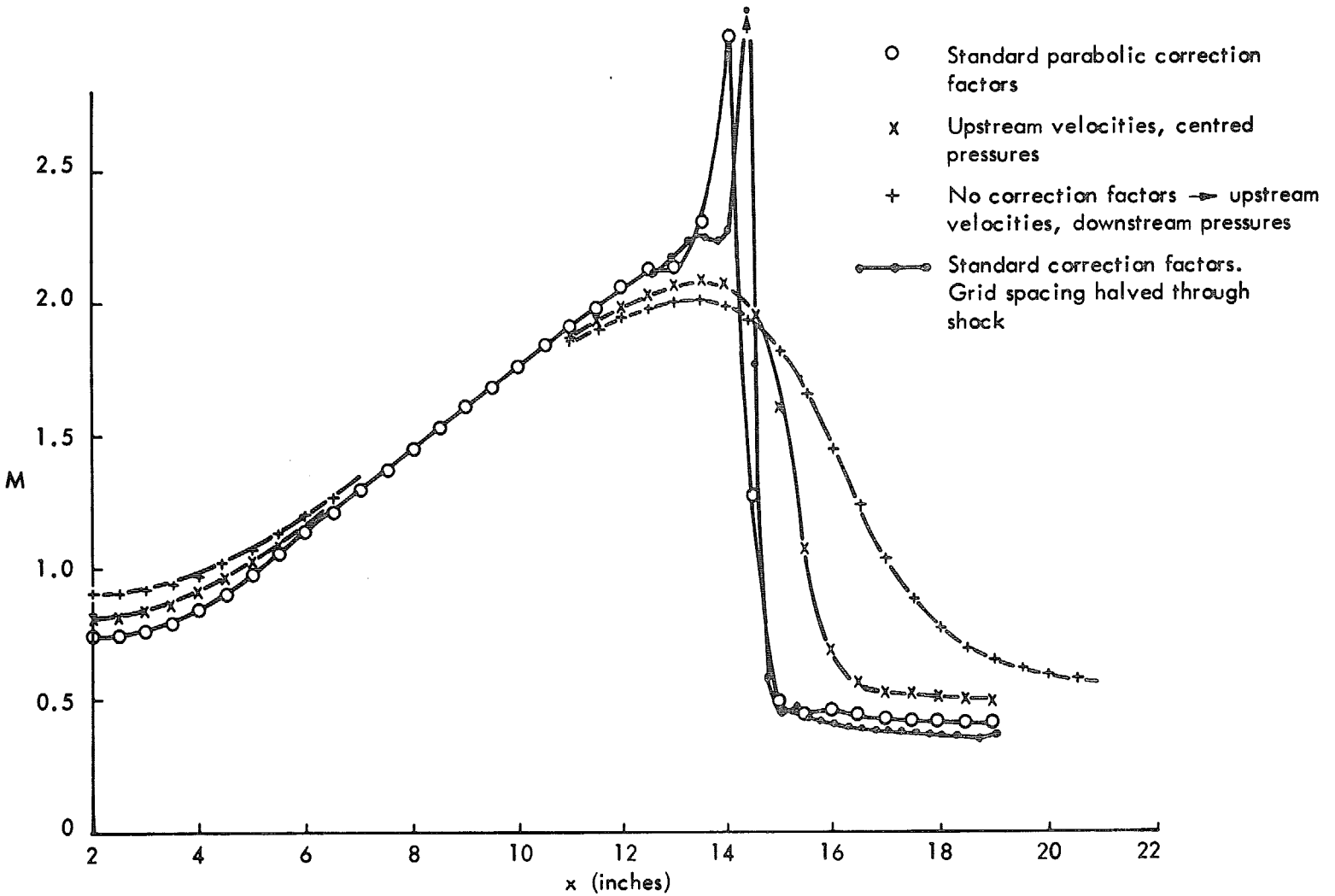

FIG. 9. Convergent—divergent nozzle. Overexpanded. Mach number on axis.

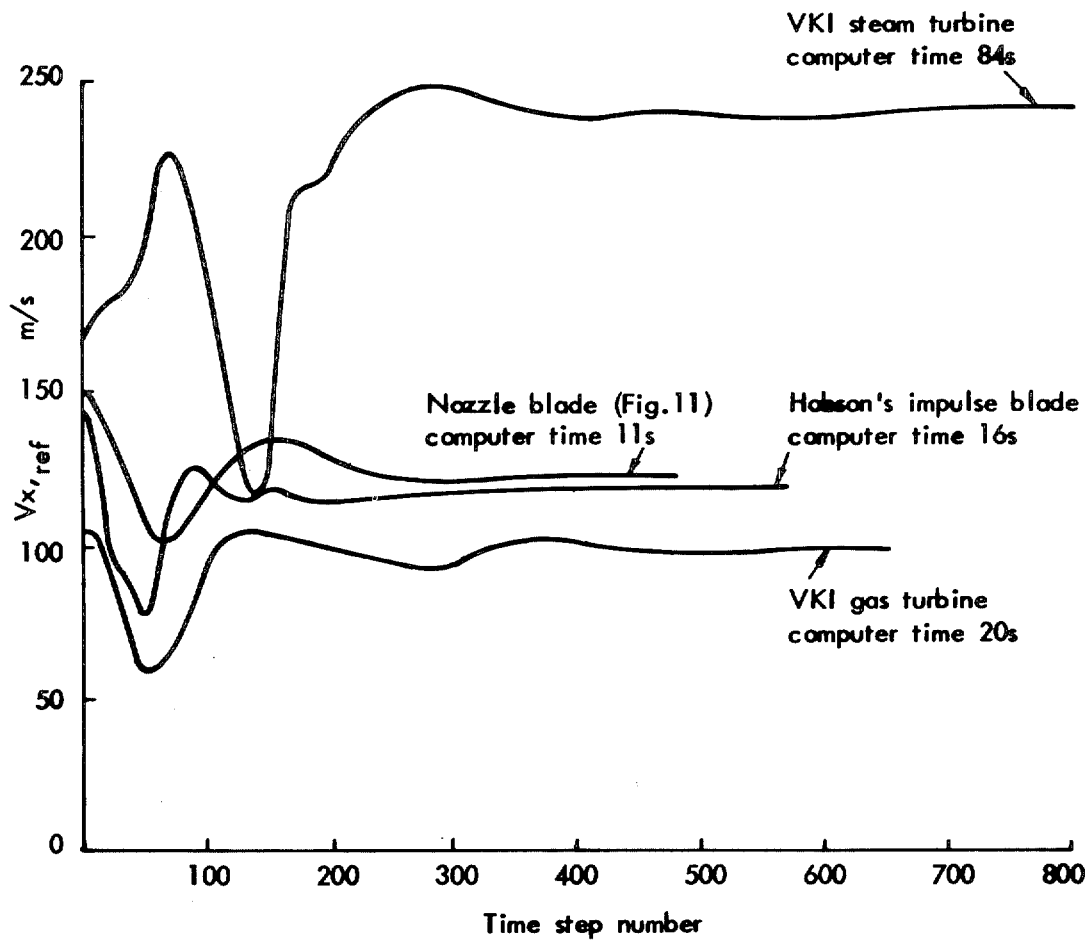

FIG. 10. Convergence of two dimensional program. $Vx_{,\text{ref}}$ = Axial velocity on suction surface just upstream of trailing edge.

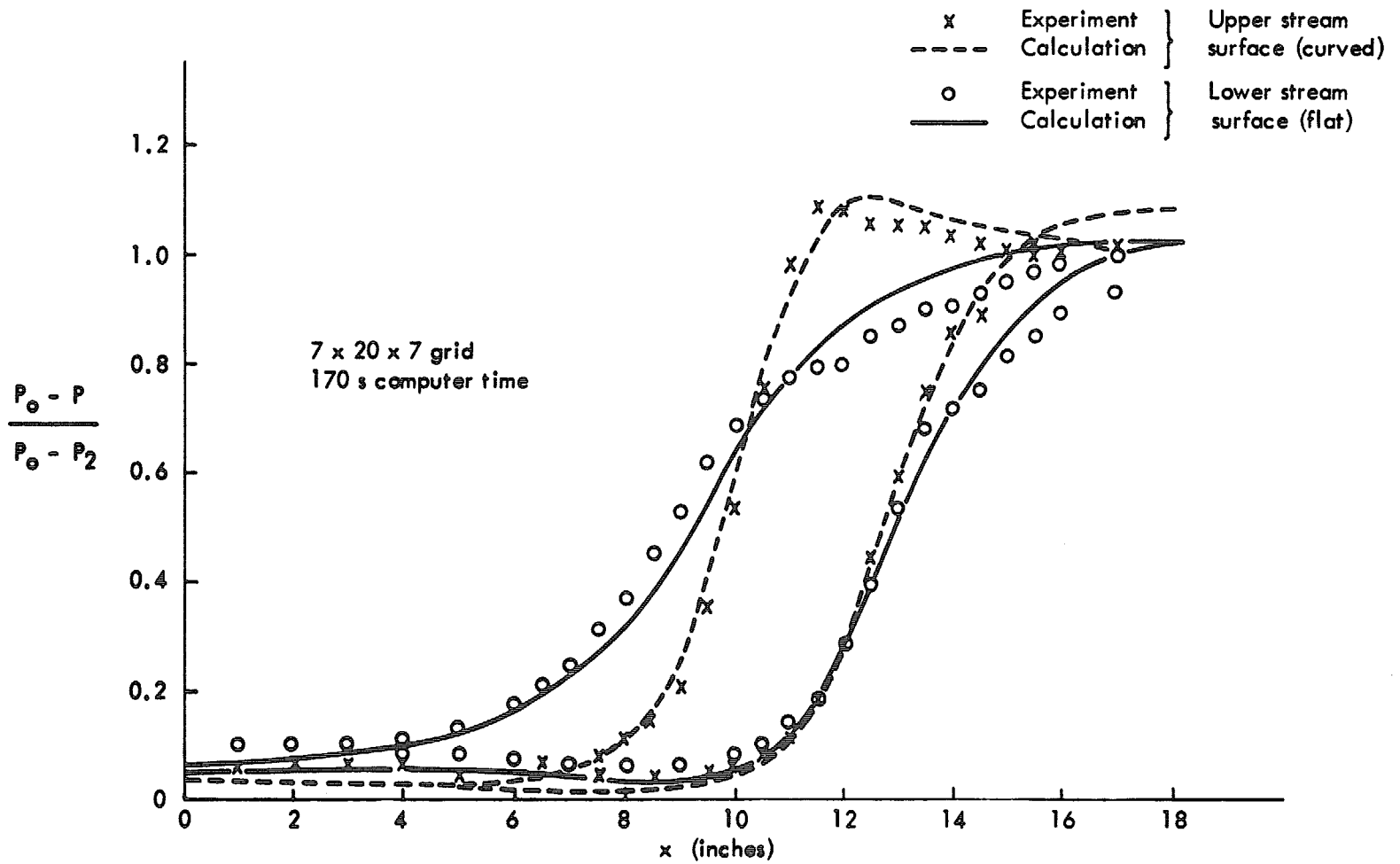

FIG. 11. Three dimensional duct.

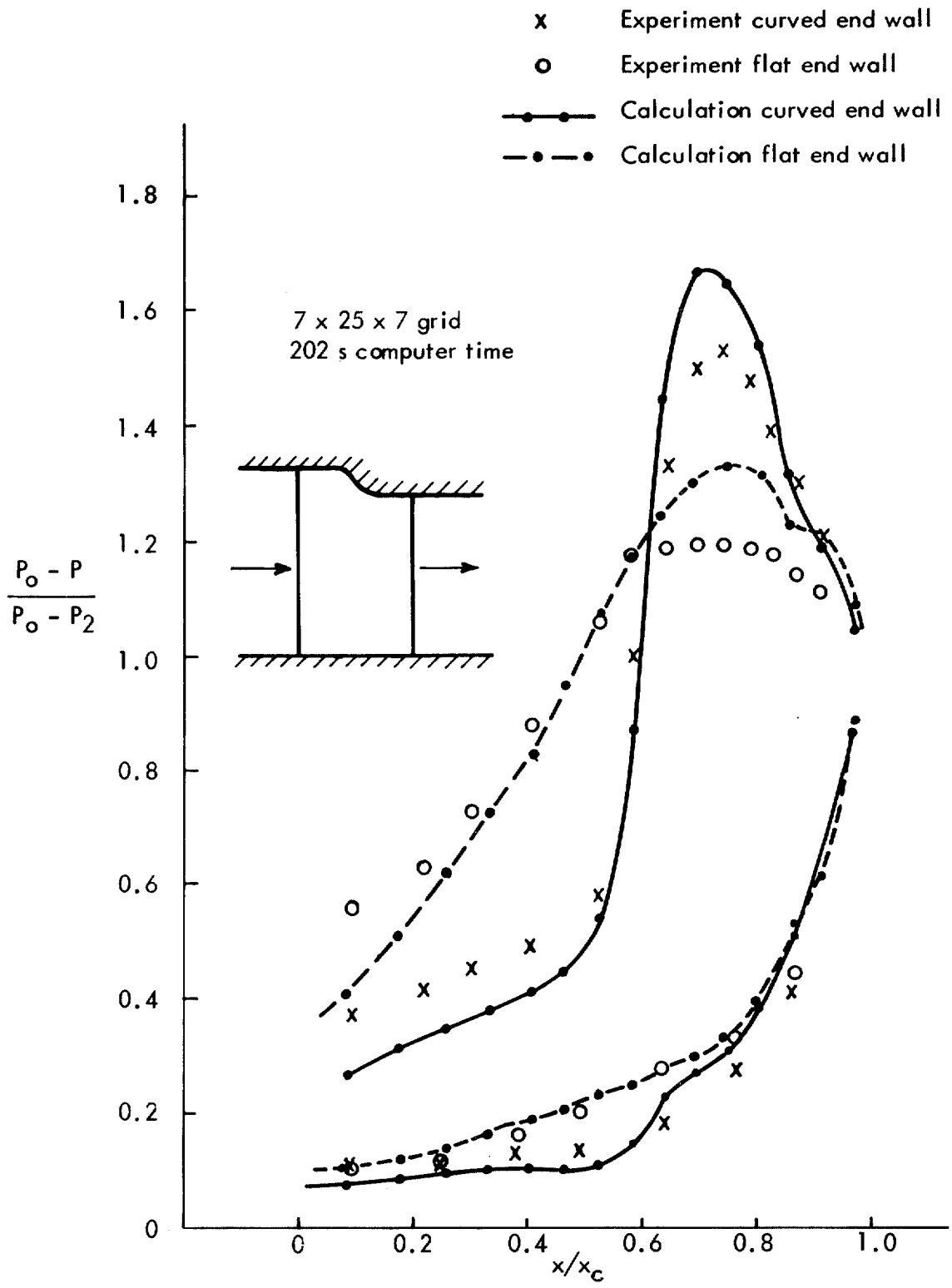

FIG. 12. Nozzle cascade with meridional profiling.

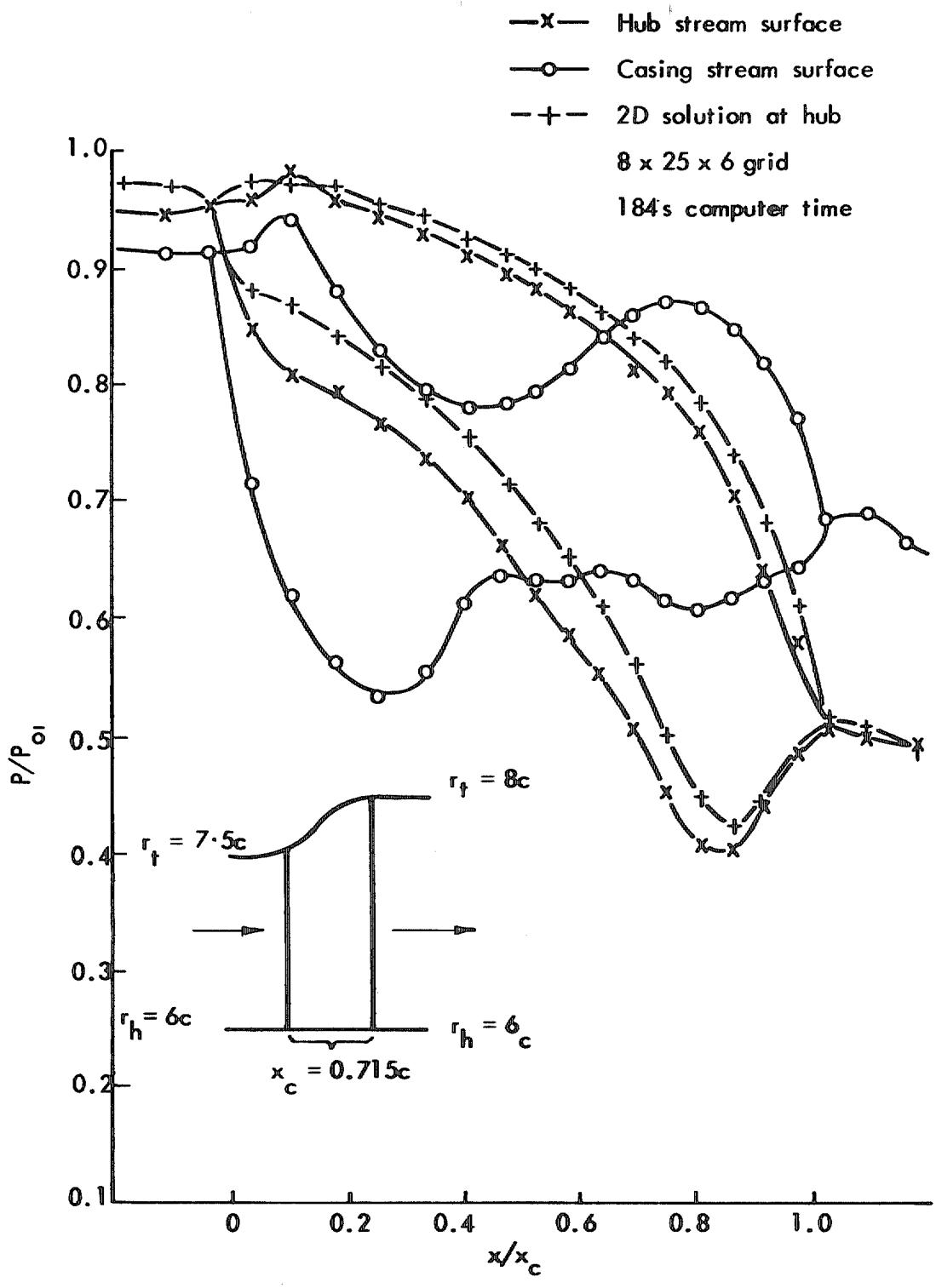

FIG. 13. 3D solution for transonic annular cascade.

Printed in England for Her Majesty's Stationery Office by J. W. Arrowsmith Ltd., Bristol BS3 2NT
Dd. 289031 K5 5/75

HER MAJESTY'S STATIONERY OFFICE

Government Bookshops

49 High Holborn, London WC1V 6HB
13a Castle Street, Edinburgh EH2 3AR
41 The Hayes, Cardiff CF1 1JW
Brazennose Street, Manchester M60 8AS
Southey House, Wine Street, Bristol BS1 2BQ
258 Broad Street, Birmingham B1 2HE
80 Chichester Street, Belfast BT1 4JY

Government publications are also available through booksellers

ISBN 0 11 470920 3